Conducting mixed-valence salt of bis(ethylenedithio)tetrathiafulvalene (BEDT-TTF) with the paramagnetic heteroleptic anion $[Cr^{III}(oxalate)_2(2,2'\text{-bipyridine})]^-$ †

Augustin M. Madalan,[ad] **Enric Canadell,**[b] **Pascale Auban-Senzier,**[c] **Diana Brânzea,**[d] **Narcis Avarvari***[a] **and Marius Andruh***[d]

Received (in Montpellier, France) 24th August 2007, Accepted 8th October 2007
First published as an Advance Article on the web 22nd October 2007
DOI: 10.1039/b713030a

The synthesis and crystal structure of the first tetrathiafulvalene (TTF) based radical cation salt containing the heteroleptic paramagnetic anion $[Cr^{III}(2,2'\text{-bipy})(C_2O_4)_2]^-$ are reported. In the salt formulated as α'-(BEDT-TTF)$_2$[Cr(C$_2$O$_4$)$_2$(2,2'-bipy)]·CHCl$_2$CH$_2$Cl according to the single-crystal X-ray structure, the BEDT-TTF (bis(ethylenedithio)tetrathiafulvalene) donors are in a mixed valence state and form two types of uniform chains within organic layers. Two overlap modes are observed in these chains, which are canted with respect to the stacking direction, leading to a peculiar α' packing mode. The anions organize in supramolecular chains sustained by π–π interactions between the bipyridine units. The magnetic behavior of the compound follows a Curie–Weiss law, with a magnetic contribution arising from both cationic and anionic counterparts. Single-crystal electrical transport measurements are in agreement with a semiconductor behavior and have been correlated with extended Hückel tight-binding calculations.

Introduction

The association of conducting and magnetic properties within tetrathiafulvalene (TTF) based radical cation salts has been providing a very active area of research in the last fifteen years.[1] Indeed, one of the main goals in the field of molecular materials is to combine within the same material at least two different physical properties, such as magnetism and conductivity, which can then coexist or interplay. A straightforward strategy to prepare such materials consists in a hybrid approach upon combination of two distinct anion and cation lattices, each furnishing a different property. Thus, in the case of TTF based salts, the organic layer, consisting in slabs of interacting TTF molecules in diverse oxidation states, exhibits conducting properties, while the anionic layer, often based on transition metal complexes, provides magnetic properties. In this respect, the bis(ethylenedithio)tetrathiafulvalene (BEDT-TTF) donor and its derivatives have afforded most of the molecular conductors or superconductors known to date.[2] It is therefore not surprising that several milestones in the field of the molecular magnetic conductors have been achieved with this family of donors.[1a] They include, for example, the synthesis of the first paramagnetic metal (BEDT-TTF)$_3$[CuCl$_4$],[3] first molecular paramagnetic superconductor (BEDT-TTF)$_4$[(H$_3$O)Fe(C$_2$O$_4$)$_3$]·PhCN ($C_2O_4^{2-}$ = oxalate),[4] first molecular ferromagnetic metal (BEDT-TTF)$_3$-[MnCr(C$_2$O$_4$)$_3$],[5] and first molecular antiferromagnetic superconductor κ-(BETS)$_2$[FeBr$_4$] (BETS = bis(ethylenedithio)tetraselenafulvalene).[6] It is worth noting that the association of BEDT-TTF with oxalate based anions gave rise to a whole family of conducting or superconducting salts formulated as (BEDT-TTF)$_4$[AM^{III}(C$_2$O$_4$)$_3$]·S (A = H_3O^+, K^+, NH_4^+; M^{III} = Cr, Fe, Co, Ga, Al; S = PhCN, PhNO$_2$, Py, PhHal, CH$_2$Cl$_2$, DMF),[4,7] although the use of other paramagnetic anions such as $[Cr^{III}(NCS)_6]^{3-}$,[8] $[Cr^{III}(NCSe)_6]^{3-}$,[9] the Reinecke type anions $[Cr^{III}(NCS)_4(L)_2]^-$ (L = NH$_3$, isoquinoline),[10] oxalate-bridged dinuclear anions $[Fe_2(C_2O_4)_5]^{4-}$,[11] or $[Cr_2(C_2O_4)(NCS)_8]^{4-}$,[12] the dithiolene based anion $[Fe^{III}(tdas)_2]^-$,[13] or, very recently, the croconate based anion $[Fe^{III}(C_5O_5)_3]^{3-}$,[14] also provided new molecular materials with the same BEDT-TTF donor.

Interestingly, most of these magnetic conducting systems contain as paramagnetic metallic centers Fe(III) or Cr(III), very often in an octahedral coordination. Note that in the case of the tris-bis(chelated) anionic complexes, such as $[M(C_2O_4)_3]^{3-}$ or $[Fe(C_5O_5)_3]^{3-}$, stereogenic centers are present as Δ and Λ enantiomers.[1a,14] In this respect, an interesting modification in the tris(oxalate) system $[M(C_2O_4)_3]^{3-}$ consists in the replacement of one oxalate dianion by one neutral 2,2'-bipyridine to afford monoanionic species such as $[Cr^{III}(2,2'\text{-bipy})(C_2O_4)_2]^-$ belonging to the more general family of $[Cr^{III}(AA)(C_2O_4)_2]^-$ complexes (AA = 2,2'-bipyridine, 1,10-phenanthroline, 2,2'-bipyrimidine, 2,2'-dipyridylamine). These compounds proved

---

[a] *Laboratoire Chimie, Ingénierie Moléculaire et Matériaux (CIMMA), UMR 6200 CNRS-Université d'Angers, UFR Sciences, Bât. K 2 Bd. Lavoisier, 49045 Angers, France. E-mail: narcis.avarvari@univ-angers.fr; Fax: (+33)02 41 73 54 05*
[b] *Institut de Ciència de Materials de Barcelona (CSIC), Campus de la UAB, E-08193 Bellaterra, Spain*
[c] *Laboratoire de Physique des Solides, UMR 8502, CNRS – Université Paris-SudBât. 510, 91405 Orsay France*
[d] *Inorganic Chemistry Laboratory, Faculty of Chemistry, University of Bucharest Str. Dumbrava Rosie nr. 23, 020464 Bucharest, Romania. E-mail: marius.andruh@dnt.ro*

† The HTML version of this article has been enhanced with colour images.

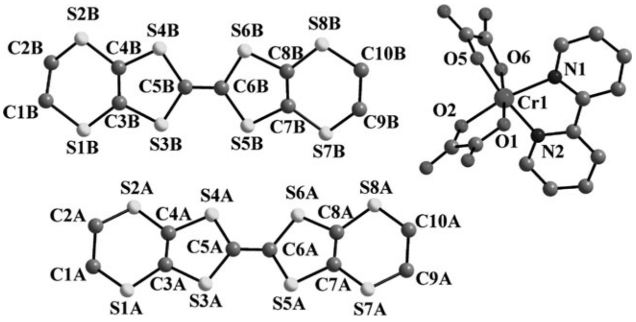

Fig. 1 Labeling scheme for the atoms of the two independent donors and the anion in compound **1**.

to be versatile building blocks for the synthesis of a large variety of solid-state structures sustained by a combination of coordinative, hydrogen bond and π–π stacking interactions.[15] Nevertheless, none of the members of this series was included so far as anionic component of molecular conductors. We report herein the synthesis, crystal structure and physical properties of the first conducting material based on the BEDT-TTF donor and $[\mathrm{Cr^{III}(2,2'\text{-bipy})(C_2O_4)_2}]^-$ anion.

Results and discussion

Synthesis and X-ray structure of α'-(BEDT-TTF)$_2$-[Cr(C$_2$O$_4$)$_2$(2,2′-bipy)]·CHCl$_2$CH$_2$Cl 1

Single crystals of the salt, as air-stable dark brown bars, have been grown by using the electrocrystallization technique,[16] in a solvent mixture $\mathrm{CH_3CN–CHCl_2CH_2Cl}$ (1 : 1), which explains the inclusion of the latter in the crystal structure. The compound crystallizes in the monoclinic system, space group $P2_1/c$, with two independent BEDT-TTF molecules, one $[\mathrm{Cr(ox)_2(2,2'\text{-bipy})}]^-$ anion and one solvent molecule (1,1,2-trichloroethane) in general positions in the unit cell (see Fig. 1 for the labeling scheme for both donor molecules and the anion).

Thus, the stoichiometry donor/anion is 2 : 1, therefore a mixed-valence type charge distribution on the donor moieties is likely to occur. The overall structure of **1** consists in alternating supramolecular layers of cations and anions along the *b* axis, within a segregated organic–inorganic architecture, as mostly often encountered in TTF based materials (Fig. 2).[2] Solvent molecules are inserted in the anionic layer, occupying voids between columns of anions.

Within the organic slabs, the two independent BEDT-TTF molecules **A** and **B** give rise to uniform homo-stacks along the *c* axis of $(\mathbf{A})_n$ and $(\mathbf{B})_n$ type, respectively, with a tilt angle of 46.2° between consecutive columns (Fig. 3(a)). The stacks are tilted with respect to the chain direction *c* by 20.6° for **A** and 25.6°, in the opposite sense, for **B**. This stacking pattern is reminiscent to the so-called α phase,[17] yet the analysis of the overlap modes between donors within the same columns reveals several peculiarities.

In the columns of donors **A** one can observe a transversal shift between successive molecules (Fig. 3(b)), a typical feature of an α phase. The shortest intermolecular intrastack S···S distance amounts to 3.939 Å for S2A···S8A(x, $0.5 - y$, $-0.5 + z$), all the others being over 4.0 Å. On the other hand, the donors **B** form also uniform stacks, overlapping each other with a combined transversal and longitudinal shift (Fig. 3(c)), unlike the typical α' phases, characterized by a sequence of transversal shift followed by a combination of transversal and longitudinal shift.[18] Once again, the intermolecular intrastack S···S distances are rather long, the shortest one, S5B···S6B(x, $0.5 - y$, $-0.5 + z$), amounting to 3.881 Å. Several other S···S distances below 4.0 Å can be also identified (*vide infra*). Thus, our compound could be classified as a peculiar α' phase, since it contains the two types of intrastack overlaps found in α' phases although in different sequences. Selected bond lengths for the donors and the anion are listed in Table 1.

The values of the central C═C bond distances suggest that the charge +1 is roughly uniformly distributed over the two donors. The analysis of the bond distances according to the method of Day and co-workers,[19] which takes into account a parameter $\delta = (\mathbf{b} + \mathbf{c}) - (\mathbf{a} + \mathbf{d})$, where **a–d** stand for the averaged values of the central C–S and C═C bonds as emphasized in Table 1, and the charge Q related to δ by the empirical equation $Q = 6.347 - 7.463\delta$, provides equal charges of $+0.65 \pm 0.1$ for both **A** and **B** donors. This result is indicative of genuine mixed-valence character of the donor lattice, without any preferential charge localization. The calculated total charge of $+1.3 \pm 0.2$ is thus in good agreement with the expected value of +1.

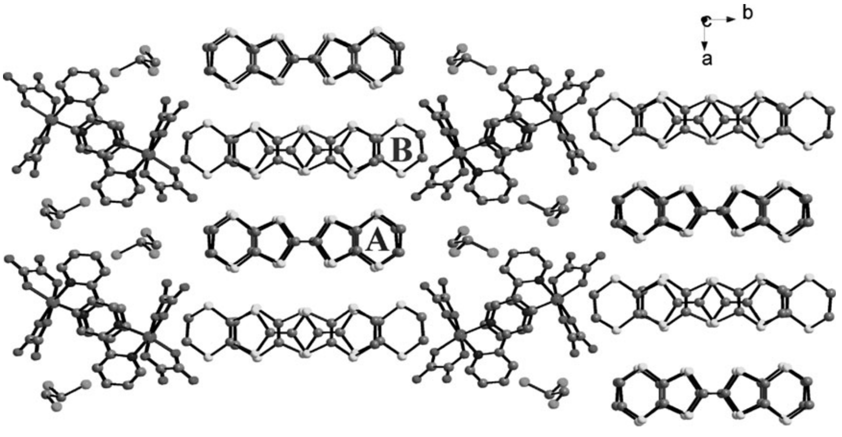

Fig. 2 View of the packing diagram along the *c* axis in crystal **1**, emphasizing the organic–inorganic segregation.

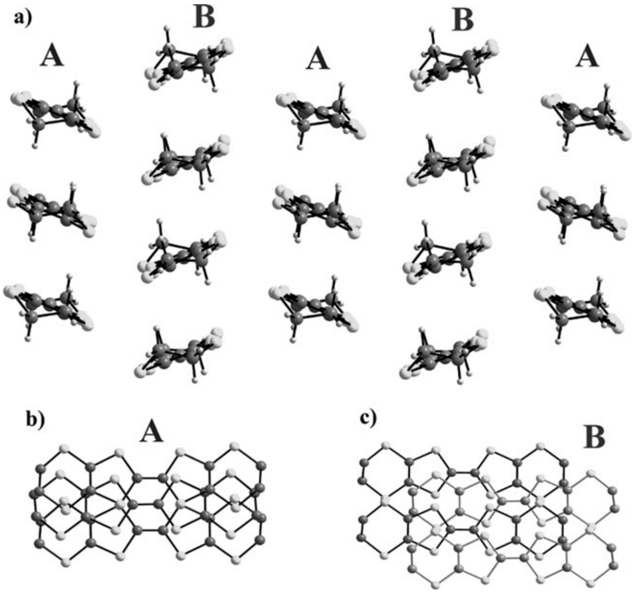

Fig. 3 View of the BEDT-TTF layers along the *b* axis (a) and projections onto the mean molecular planes of the **A** and **B** stacks (b and c) which emphasize the intrastack overlap modes.

The $[Cr(ox)_2(2,2'\text{-bipy})]^-$ anions form supramolecular zig-zag chains running along the *c* axis, separated by trichloroethane molecules, upon π–π interactions established between 2,2′-bipyridine molecules (Fig. 4(a)). Two types of π–π contacts **I** (Fig. 4(b)) and **II** (Fig. 4(c)) can be disclosed, associated with short intermolecular C···C or C···N distances of 3.55–3.81 Å for **I** and 3.27–3.57 Å for **II**, respectively.

The chromium ions exhibit octahedral coordination stereochemistry with two oxalate anions and one neutral 2,2′-bipyridine molecule acting as chelating ligands. The Cr–O distances vary between 1.932(4) and 1.952(4) Å, while the Cr–N distances are longer, amounting to 2.069(5) and 2.072(4) Å (Table 1), all of them ranging in the usual values observed for this anion.[15] The shortest Cr···Cr distances are as long as 7.510 Å for Cr1···Cr1(−*x*, −*y*, −*z*) within the π–π dyad **I** and 7.855 Å for Cr1···Cr1(−*x*, −*y*, 1 − *z*) in **II**, therefore any direct magnetic exchange coupling between paramagnetic Cr centers is very likely precluded. The anions exist as Δ and Λ enantiomers which alternate through inversion centers along the supramolecular chains, which are thus heterochiral.

Table 1 Selected bond lengths (Å) for **1**

Compound	1	
	A	B
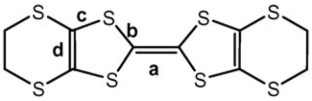		
a	1.374(8)	1.364(7)
b	1.736(6)	1.742(5)
	1.726(6)	1.735(5)
	1.729(6)	1.732(5)
	1.740(6)	1.738(5)
c	1.749(5)	1.748(5)
	1.748(6)	1.748(5)
	1.752(6)	1.732(5)
	1.748(5)	1.741(5)
d	1.350(8)	1.355(7)
	1.339(8)	1.350(7)
Cr1–O1	1.952(4)	
Cr1–O2	1.932(4)	
Cr1–O5	1.943(4)	
Cr1–O6	1.942(4)	
Cr1–N1	2.072(4)	
Cr1–N2	2.069(5)	

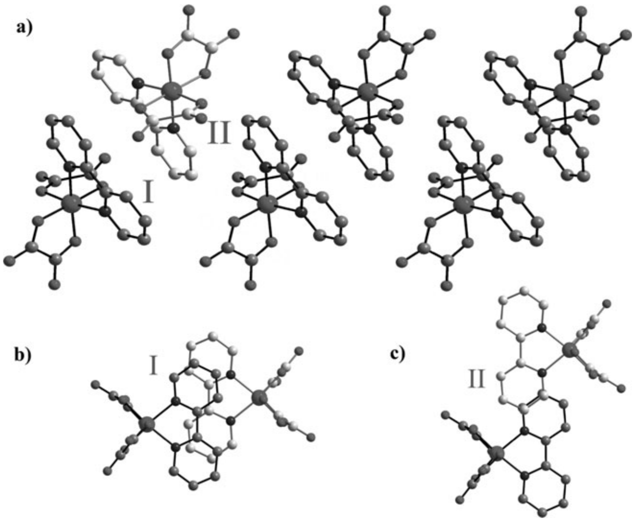

Fig. 4 View of the supramolecular chains formed by $[Cr(ox)_2(2,2'\text{-bipy})]^-$ anions (a) and details of the π–π stacking interactions (b and c).

Magnetic and electrical transport properties. Band structure calculation

The magnetic properties of the mixed-valence salt **1**, plotted as χ*T* product *vs.* *T* (χ = molar magnetic susceptibility per chromium atom) are shown in Fig. 5.

The room-temperature value of the product χ*T* amounts to 2.14 $cm^3\ mol^{-1}$ K, therefore, when subtracting the major

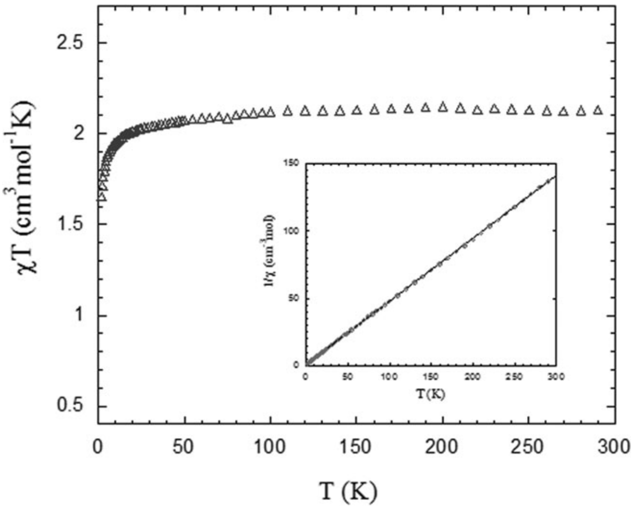

Fig. 5 χ*T* *vs.* *T* plot at 5000 Oe for α′-$(BEDT\text{-}TTF)_2[Cr(C_2O_4)_2(2,2'\text{-bipy})]\cdot CHCl_2CH_2Cl$ **1**. The inset shows the 1/χ *vs.* *T* plot. The solid line represents the best fit curve.

contribution to the susceptibility provided by the chromium ions alone ($S = 3/2$), for which a value of 1.876 cm^3 mol^{-1} K is expected,[15c,f] the contribution of BEDT-TTF molecules is 0.264 cm^3 mol^{-1} K (with an average of 0.132 cm^3 mol^{-1} K for each BEDT-TTF donor). This value, corresponding to a 70% contribution of the spin-only value for $S = 1/2$ per two BEDT-TTF, definitely shows that the donor molecules are not dimerized or strongly antiferromagnetically coupled at room temperature, in agreement with the structural analysis (*vide supra*). Note that contributions at different extents from the organic donors in TTF-based radical cation salts, with chromium containing anions, are not uncommon and depend on the degree of dimerization, antiferromagnetic exchange interactions and electron delocalization through the organic layer.[9,10b,20] The product χT remains practically constant from room temperature down to 50 K, then it starts to decrease slowly down to 20 K, and, upon further cooling, a much more rapid decrease is observed down to 2.0 K, temperature at which the product χT reaches the value of 1.62 cm^3 mol^{-1} K. As already evoked in the case of compounds containing only [Cr(ox)$_2$(2,2′-bipy)]$^-$ anions as spin carriers and presenting roughly the same behavior,[15c,f] the deviation from the Curie law at low temperatures can be imputable to the zero field splitting (D) of the ground state of Cr^{III} and/or to weak antiferromagnetic superexchange chromium–chromium interactions, very likely mediated by π–π overlaps between 2,2′-bipy rings. In the case of our salt, an additional source of magnetic susceptibility loss could be also the enhancement of the antiferromagnetic interactions between organic radicals. However, the magnetic susceptibility data can be well fitted by the Curie–Weiss law with a Curie constant of 2.14 cm^3 mol^{-1} K and a Weiss temperature θ of −1.11 K (inset Fig. 5).

The temperature dependence of the four-probe resistivity (ρ) measured on a single crystal along the most conductive direction is consistent with a semiconducting character for the compound **1**. The plot of log(ρ) *vs.* T^{-1} (Fig. 6) shows linear behaviors above 250 K and below 200 K associated with two different activation energies which can be estimated to 0.31 eV (3600 K) (calculated between 300 and 250 K) and 0.12 eV (1400 K) (calculated between 200 and 100 K). The room-temperature value of the conductivity, σ(300 K), amounts to 0.5 S cm^{-1}, which is typical for a good semiconductor with a rather small gap or with electron localization.

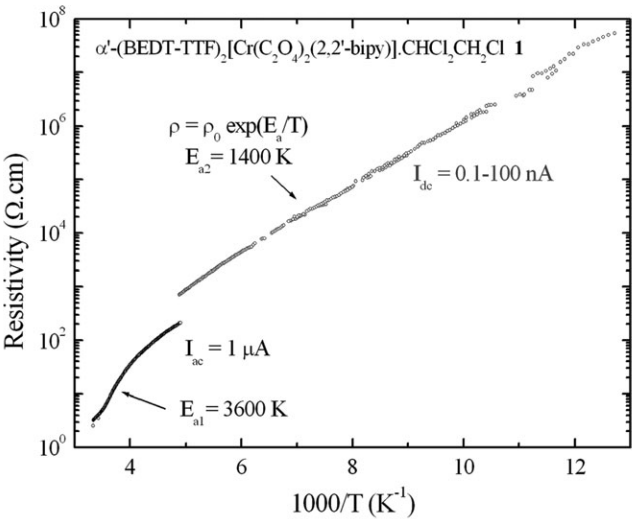

Fig. 6 Single-crystal resistivity measurements for α′-(BEDT-TTF)$_2$-[Cr(C$_2$O$_4$)$_2$(2,2′-bipy)]·CHCl$_2$CH$_2$Cl **1**.

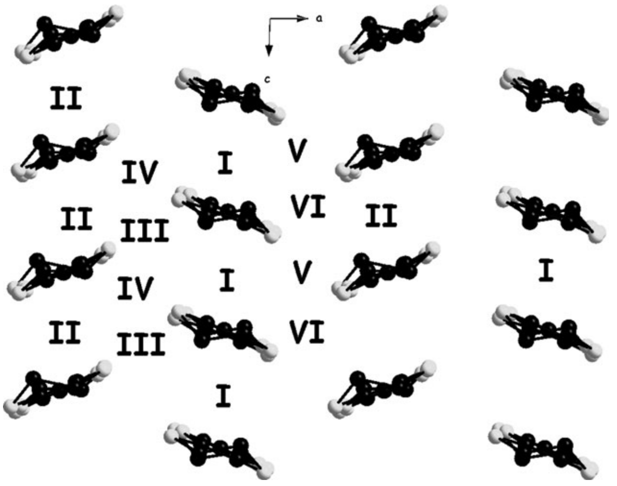

Fig. 7 Donor–donor interactions in the organic layer.

In order to have a deeper understanding of the electronic interactions occurring in the organic layer we have undertaken extended Hückel calculations to determine the intermolecular $\beta_{\text{HOMO–HOMO}}$ interaction energies between the closest BEDT-TTF neighbors. Two intrastack (**I** and **II**) and four interstack (**III**–**VI**) donor–donor interactions have been identified (Fig. 7). The absolute values of the calculated $\beta_{\text{HOMO–HOMO}}$ energies along with the corresponding short S···S contacts are listed in Table 2. Although lateral interactions **III**–**VI** are, in average, stronger than the intrachain ones (**I** and **II**), a normal characteristic for the family of α′ phases, their magnitude is globally rather small when compared with those of typical α′ phases.[18] This is indicative of weak band dispersion, and hence electron localization.

Tight-binding calculations afforded the band structure diagram shown in Fig. 8. Because of the stoichiometry, these bands must accommodate two holes.

The overall topology of this band structure is typical of that of α′ phases, as for example the (BEDT-TTF)$_4$PtBr$_6$ salt,[21] which was found to be a semiconductor. Indeed, according to the band structure calculations for this compound, the two upper HOMO bands are very narrow, and, even though there is no band gap in between, the system exhibits an activated, semiconducting behaviour, because of electron localization. In

Table 2 Intermolecular interactions associated to S···S contacts shorter than 4 Å, with the corresponding absolute values of the interaction energies $|\beta_{\text{HOMO–HOMO}}|$

Interaction	S···S (<4.0 Å)	$\lvert\beta_{\text{HOMO–HOMO}}\rvert$/eV
I (A–A)	3.939	0.0451
II (B–B)	3.881, 3.911, 3.967, 3.985, 3.998	0.0747
III (A–B)	3.536, 3.674, 3.739, 3.895, 3.910	0.0529
IV (A–B)	3.419, 3.607, 3.784, 3.911, 3.996	0.0994
V (A–B)	3.608, 3.652, 3.717, 3.870, 3.873, 3.883	0.0934
VI (A–B)	3.423, 3.659, 3.726, 3.848	0.0525

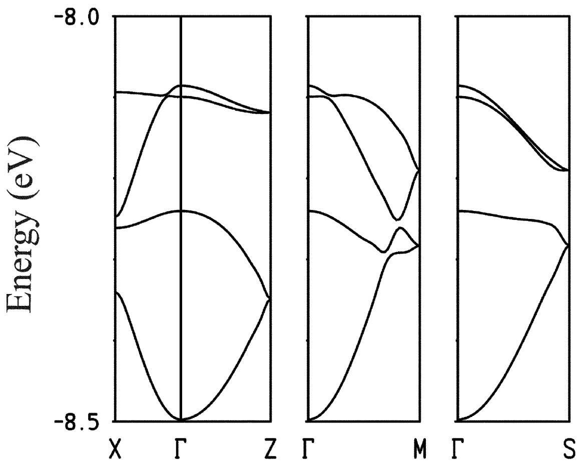

Fig. 8 Calculated band structure for α′-(BEDT-TTF)$_2$-[Cr(C$_2$O$_4$)$_2$(2,2′-bipy)]·CHCl$_2$CH$_2$Cl **1**: Γ = (0, 0), X = (a*/2, 0), Z = (0, c*/2), M = (a*/2, c*/2) and S = (−a*/2, c*/2).

our salt neither there is a band gap between the third and the fourth band (Fig. 8), and therefore the compound is clearly not a band gap semiconductor. Nevertheless, the total dispersion of the bands is even about 27% weaker than that of (BEDT-TTF)$_4$PtBr$_6$ salt, therefore the intersite repulsions very likely dominate over the band dispersion, thus leading to a localized system. Moreover, since there is only one interaction value along each chain, there is no possibility to form clearly defined dimers, unlike the cases of (BEDT-TTF)$_4$PtBr$_6$ salt and other α′ phases. Hence, the place where the electrons localize is not evident here, and that still remains an open question. In this respect, the newly synthesized α′ phase (BEDT-TTF)$_2$[Cr(C$_2$O$_4$)$_2$(2,2′-bipy)] is clearly original both structurally and electronically, and we feel that additional physical measurements, such as conductivity under pressure, could afford further interesting results.

Conclusion

In summary, we have synthesized upon electrocrystallization the new paramagnetic semiconductor α′-(BEDT-TTF)$_2$-[Cr(oxalate)$_2$(2,2′-bipy)]·CHCl$_2$CH$_2$Cl, which shows a typical organic–inorganic segregation in its crystal structure. The paramagnetic anions, containing octahedrally coordinated chromium(III) ions, organize in supramolecular chains sustained by π–π interactions between adjacent bipy units. The organic donors, each bearing a mean charge of +0.5, organize in uniform chains tilted with respect to each other, forming a peculiar α′ slab. Accordingly, larger interchains than intrachain HOMO–HOMO interactions have been calculated. The magnetic response of the compound is mainly dominated by the paramagnetism of the Cr^{III} S = 3/2 ions, although the contribution of the organic donors is sizeable, and can be modeled by a Curie–Weiss law. The transport properties, investigated by single-crystal resistivity measurements, demonstrate a semiconducting behavior, very likely due to electron localization, as suggested by the weak dispersion of the energy bands. Moreover, the band structure calculations, using the extended Hückel method, rule out the possibility of a band gap semiconductor. The salt we describe herein represents a new member of the growing family of the molecular paramagnetic conductors and the first one containing the heteroleptic anion [Cr(oxalate)$_2$(2,2′-bipy)]$^-$.

Experimental

Synthesis

Dark brown prisms of α′-(BEDT-TTF)$_2$[Cr(C$_2$O$_4$)$_2$(2,2′-bipy)]·CHCl$_2$CH$_2$Cl (**1**) were obtained by electrocrystallization as follows. (PPh$_4$)[Cr(oxalate)$_2$(2,2′-bipy)] (70.0 mg), prepared by paralleling the synthesis of (AsPh$_4$)[Cr(oxalate)$_2$(2,2′-bipy)] described in the literature,[15c] was dissolved in a mixture of CH$_3$CN (7 mL) and CHCl$_2$CH$_2$Cl (7 mL). In a half of this solution BEDT-TTF (8.0 mg) was added, and then the suspension was placed in the anodic chamber of the electrocrystallization cell, while the other half containing only the supporting electrolyte was poured in the cathodic compartment. Single crystals of the salt were grown at 27 °C over a period of 14 days on a platinum wire electrode, by applying a constant current of 1 μA.

X-Ray crystal structure determinations

Details about data collection and solution refinement are given in Table 3. X-Ray diffraction measurements were performed on a Stoe Imaging Plate System operating with a Mo-Kα (λ = 0.71073 Å) X-ray tube with a graphite monochromator. The structure was solved (SHELXS-97) by direct methods and refined (SHELXL-97) by full-matrix least-square procedures on F^2.[22] All non-H atoms were refined anisotropically, and hydrogen atoms were introduced at calculated positions (riding model), included in structure factor calculations but not refined.

CCDC reference number 663262.

For crystallographic data in CIF or other electronic format see DOI: 10.1039/b713030a

Table 3 Crystallographic data, details of data collection and structure refinement parameters for **1**

Compound	**1**
Chemical formula	C$_{36}$H$_{27}$Cl$_3$CrN$_2$O$_8$S$_{16}$
M/g mol^{-1}	1286.91
T/K	293(2)
λ/Å	0.71073
Crystal system	Monoclinic
Space group	$P2_1/c$
a/Å	11.4268(6)
b/Å	51.0126(19)
c/Å	8.3365(5)
β/°	91.829(7)
V/Å^3	4857.0(4)
Z	4
D_c/g cm^{-3}	1.760
μ/mm^{-1}	1.141
F(000)	2608
Goodness-of-fit on F^2	0.998
Final R_1, wR_2 [$I > 2\sigma(I)$]	0.0656, 0.1553
R_1, wR_2 (all data)	0.1013, 0.1757
$\Delta\rho_{max,min}$/e Å^{-3}	0.695, −0.532

Magnetic measurements

The variable-temperature magnetic susceptibility measurements were obtained with the use of a Quantum Design SQUID magnetometer MPMS-XL. Measurements were performed on a finely ground crystalline sample of **1** (11.83 mg). The magnetic data were corrected for the diamagnetic contribution of the sample and the sample holder, estimated from the Pascal's constants.[23]

Single-crystal conductivity measurements

Electrical resistivity was measured on prismatic shaped crystals of **1**. Gold contacts were evaporated on the crystals and gold wires were glued with silver paste on those contacts. Resistivity measurements were performed in the range 80–300 K with a four point method. A low frequency ($<$100 Hz) lock-in technique with a measuring current I_{ac} = 1 μA was used for resistance values lower than 50 kΩ, while higher resistances were measured with dc currents ranging from 100 to 0.1 nA.

Band structure calculations

The tight-binding band structure calculations were of the extended Hückel type[24a] with a modified Wolfsberg–Helmholtz formula to calculate the non-diagonal $H_{\mu\nu}$ values.[24b] The basis set consisted of double-ζ Slater-type orbitals for C and S and single-ζ Slater-type orbitals for H. The exponents, contraction coefficients and ionization potentials were taken from previous work.[25]

Acknowledgements

Financial support from Région Pays de la Loire (grant to A. M. M.) and from French Ministry of Foreign Affairs through a BRANCUSI (PAI 08794NE) project is gratefully acknowledged. This work was also supported by CNRS (France), a CNRS-Académie Roumaine project (Project 17013), and by MEC-Spain (Project FIS2006-12117-C04-01) and Generalitat de Catalunya (Project 2005 SGR 683).

References

1 (*a*) E. Coronado and P. Day, *Chem. Rev.*, 2004, **104**, 5419–5448; (*b*) E. Coronado and J. R. Galán-Mascarós, *J. Mater. Chem.*, 2005, **15**, 66–74; (*c*) L. Ouahab and T. Enoki, *Eur. J. Inorg. Chem.*, 2004, 933–941; (*d*) P. Day and M. Kurmoo, *J. Mater. Chem.*, 1997, **7**, 1291–1295.

2 (*a*) J. M. Williams, J. R. Ferraro, R. J. Thorn, K. D. Carlson, U. Geiser, H. H. Wang, A. M. Kini and M.-H. Whangbo, in *Organic Superconductors (Including Fullerenes), Synthesis, Structure, Properties and Theory*, ed. R. N. Grimes, Prentice-Hall, Englewoods Cliffs, NJ, 1992; (*b*) T. Ishiguro, K. Yamaji and G. Saito, *Organic Superconductors*, Spinger-Verlag, Heidelberg, Germany, 1998.

3 P. Day, M. Kurmoo, T. Mallah, I. R. Marsden, R. H. Friend, F. L. Pratt, W. Hayes, D. Chasseau, J. Gaultier, G. Bravic and L. Ducasse, *J. Am. Chem. Soc.*, 1992, **114**, 10722–10729.

4 (*a*) A. W. Graham, M. Kurmoo and P. Day, *J. Chem. Soc., Chem. Commun.*, 1995, 2061–2062; (*b*) M. Kurmoo, A. W. Graham, P. Day, S. J. Coles, M. B. Hursthouse, J. L. Caulfield, J. Singleton, F. L. Pratt, W. Hayes, L. Ducasse and P. Guionneau, *J. Am. Chem. Soc.*, 1995, **117**, 12209–12217.

5 E. Coronado, J. R. Galán-Mascarós, C. J. Gómez-García and V. Laukhin, *Nature*, 2000, **408**, 447–449.

6 (*a*) H. Kobayashi, H. B. Cui and A. Kobayashi, *Chem. Rev.*, 2004, **104**, 5265–5288; (*b*) H. Fujiwara, E. Fujiwara, Y. Nakazawa, B. Z. Narymbetov, K. Kato, H. Kobayashi, A. Kobayashi, M. Tokumoto and P. Cassoux, *J. Am. Chem. Soc.*, 2001, **123**, 306–314.

7 (*a*) L. Martin, S. S. Turner, P. Day, F. E. Mabbs and E. J. L. McInnes, *Chem. Commun.*, 1997, **12**, 1367–1368; (*b*) L. Martin, S. S. Turner, P. Day, P. Guionneau, J. A. K. Howard, D. E. Hibbs, M. E. Light, M. B. Hursthouse, M. Uruichi and K. Yakushi, *Inorg. Chem.*, 2001, **40**, 1363–1371; (*c*) H. Akutsu, A. Akutsu-Sato, S. S. Turner, D. Le Pévelen, P. Day, V. Laukhin, A.-K. Klehe, J. Singleton, D. A. Tocher, M. R. Probert and J. A. K. Howard, *J. Am. Chem. Soc.*, 2002, **124**, 12430–12431; (*d*) E. Coronado, S. Curreli, C. Giménez-Saiz and C. J. Gómez-García, *Synth. Met.*, 2005, **154**, 245–248; (*e*) E. Coronado, S. Curreli, C. Giménez-Saiz and C. J. Gómez-García, *J. Mater. Chem.*, 2005, **15**, 1429–1436; (*f*) T. G. Prokhorova, S. S. Khasanov, L. V. Zorina, L. I. Buravov, V. A. Tkacheva, A. A. Baskakov, R. B. Morgunov, M. Gener, E. Canadell, R. P. Shibaeva and E. B. Yagubskii, *Adv. Funct. Mater.*, 2003, **13**, 403–411.

8 F. Bérézovsky, S. Triki, J. Sala Pala, J. R. Galán-Mascarós, C. J. Gómez-García and E. Coronado, *Synth. Met.*, 1999, **102**, 1755–1756.

9 S. S. Turner, D. Le Pévelen, P. Day and K. Prout, *J. Solid State Chem.*, 2002, **168**, 573–581.

10 (*a*) C. J. Kepert, M. Kurmoo, M. R. Truter and P. Day, *J. Chem. Soc., Dalton Trans.*, 1997, 607–613; (*b*) S. S. Turner, C. Michaut, S. Durot, P. Day, T. Gelbrich and M. B. Hursthouse, *J. Chem. Soc., Dalton Trans.*, 2000, 905–909.

11 S. Rashid, S. S. Turner, P. Day, M. E. Light and M. B. Hursthouse, *Inorg. Chem.*, 2000, **39**, 2426–2428.

12 S. Triki, F. Bérézovsky, J. Sala Pala, C. J. Gómez-García, E. Coronado, K. Costuas and J.-F. Halet, *Inorg. Chem.*, 2001, **40**, 5127–5132.

13 P. Deplano, L. Leoni, M. L. Mercuri, J. A. Schlueter, U. Geiser, H. H. Wang, A. M. Kini, J. L. Manson, C. J. Gómez-García, E. Coronado, H.-J. Koo and M.-H. Whangbo, *J. Mater. Chem.*, 2002, **12**, 3570–3577.

14 (*a*) C. J. Gómez-García, E. Coronado, S. Curreli, Carlos Giménez-Saiz, P. Deplano, M. L. Mercuri, L. Pilia, A. Serpe, C. Faulmann and E. Canadell, *Chem. Commun.*, 2006, **12**, 4931–4933; (*b*) E. Coronado, S. Curreli, Carlos Giménez-Saiz, C. J. Gómez-García, P. Deplano, M. L. Mercuri, A. Serpe, L. Pilia, C. Faulmann and E. Canadell, *Inorg. Chem.*, 2007, **46**, 4446–4457.

15 (*a*) M. Andruh, R. Melanson, C. V. Stager and F. D. Rochon, *Inorg. Chim. Acta*, 1996, **251**, 309–317; (*b*) F. D. Rochon, R. Melanson and M. Andruh, *Inorg. Chem.*, 1996, **35**, 6086–6092; (*c*) M. C. Muñoz, M. Julve, F. Lloret, J. Faus and M. Andruh, *J. Chem. Soc., Dalton Trans.*, 1998, **12**, 3125–3131; (*d*) G. Marinescu, M. Andruh, R. Lescouëzec, M. C. Muñoz, J. Cano, F. Lloret and M. Julve, *New J. Chem.*, 2000, **24**, 527–536; (*e*) G. Marinescu, C. Ovezea, N. Avarvari and M. Andruh, *Rev. Roum. Chim.*, 2004, **49**, 221–226; (*f*) G. Marinescu, M. Andruh, M. Julve, F. Lloret, R. Llusar, S. Uriel and J. Vaissermann, *Cryst. Growth Des.*, 2005, **5**, 261–267.

16 (*a*) T. J. Emge, H. H. Wang, M. A. Beno, J. M. Williams, M. H. Whangbo and M. Evain, *J. Am. Chem. Soc.*, 1986, **108**, 8215–8223; (*b*) P. Batail, K. Boubekeur, M. Fourmigué and J.-C. P. Gabriel, *Chem. Mater.*, 1998, **10**, 3005–3015.

17 T. Mori, H. Mori and S. Tanaka, *Bull. Chem. Soc. Jpn.*, 1999, **72**, 179–197.

18 S. V. Simonov, I. Yu. Shevyakova, L. V. Zorina, S. S. Khasanov, L. I. Buravov, V. A. Emel'yanov, E. Canadell, R. P. Shibaeva and E. B. Yagubskii, *J. Mater. Chem.*, 2005, **15**, 2476–2488.

19 P. Guionneau, C. J. Kepert, G. Bravic, D. Chasseau, M. R. Truter, M. Kurmoo and P. Day, *Synth. Met.*, 1997, **86**, 1973–1974.

20 (*a*) S. Wang, P. Day, L. M. Toma, M. Julve and J. D. Wallis, *Inorg. Chim. Acta*, 2006, **359**, 3283–3290; (*b*) K. Hervé, O. Cador, S. Golhen, K. Costuas, J.-F. Halet, T. Shirahata, T. Muto, T. Imakubo, A. Miyazaki and L. Ouahab, *Chem. Mater.*, 2006, **18**, 790–797.

21 R. Rousseau, M.-L. Doublet, E. Canadell, R. P. Shibaeva, S. S. Khasanov, L. P. Rozenberg, N. D. Khusch and E. B. Yagubskii, *J. Phys. I Fr.*, 1996, **6**, 1527–1553.

22 G. M. Sheldrick, *Programs for the Refinement of Crystal Structures*, University of Göttingen, Göttingen, Germany, 1996.

23 E. A. Boudreaux and L. N. Mulay, in *Theory and Applications of Molecular Magnetism*, John Wiley & Sons, New York, 1976.

24 (*a*) M.-H. Whangbo and R. Hoffmann, *J. Am. Chem. Soc.*, 1978, **100**, 6093–6098; (*b*) J. H. Ammeter, H.-B. Bürgi, J. Thibeault and R. Hoffmann, *J. Am. Chem. Soc.*, 1978, **100**, 3686–3692.

25 A. Pénicaud, K. Boubekeur, P. Batail, E. Canadell, P. Auban-Senzier and D. Jérome, *J. Am. Chem. Soc.*, 1993, **115**, 4101–4112.